

# Higher-order soft and virtual corrections in $pp \rightarrow \gamma W$ production at the LHC

Nikolaos Kidonakis<sup>a</sup> and Alberto Tonerio<sup>a,b</sup>

<sup>a</sup>*Department of Physics, Kennesaw State University,  
Kennesaw, GA 30144, USA*

<sup>b</sup>*Department of Chemistry and Physics, Florida Gulf Coast University,  
Fort Myers, FL 33965, USA*

## Abstract

We study higher-order QCD corrections beyond NLO for the associated production of a photon with a  $W$  boson ( $\gamma W^+$  and  $\gamma W^-$  production) at the Large Hadron Collider. We calculate the NNLO soft-plus-virtual QCD corrections as well as the N<sup>3</sup>LO soft-gluon corrections to the total production cross section and the photon transverse-momentum distribution in single-particle-inclusive kinematics. The higher-order corrections provide a significant enhancement to the cross section. This is the first calculation of the complete soft-gluon corrections at N<sup>3</sup>LO in single-particle-inclusive kinematics for a Standard Model process.

## 1 Introduction

The associated production of a photon with a  $W$  boson ( $\gamma W^+$  and  $\gamma W^-$ ) has been studied experimentally and theoretically for a long time at relevant collider energies. The interest in these processes is in part due to the possibility of probing the triple gauge coupling of a photon with two  $W$  bosons since such diagrams already contribute at lowest order in addition to diagrams with photon and  $W$  couplings to quark lines. Thus, measurements of the  $\gamma W$  cross section can be used to look for effects of new physics and set limits on anomalous gauge couplings.

The  $\gamma W$  production cross section was first measured in 1.8 TeV [1–3] and 1.96 TeV [4–7] proton-antiproton collisions at the Tevatron. It was later studied in proton-proton collisions at the LHC at 7 TeV [8–12], 8 TeV [13], and 13 TeV [14–16] energies.

Theoretical studies for  $\gamma W$  production have appeared at various orders in Refs. [17–26]. The leading-order (LO) calculation was done in [17], the next-to-leading-order (NLO) QCD corrections were calculated in [18], the next-to-next-to-leading-order (NNLO) soft-plus-virtual QCD corrections were calculated in [19], and the NNLO QCD corrections were presented in [26].

Soft-gluon corrections are important for a wide variety of processes in the Standard Model and beyond because the production cross sections receive large contributions from soft-gluon emission near partonic threshold. In this work, we calculate the soft-gluon corrections through next-to-next-to-next-to-leading-order (N<sup>3</sup>LO) based on the general resummation formalism in Refs. [27–39] and using single-particle-inclusive kinematics with the photon as the identified particle. We present approximate NNLO (aNNLO) and approximate N<sup>3</sup>LO (aN<sup>3</sup>LO) total and differential cross sections to  $\gamma W$  production. The aNNLO theoretical predictions are derived by adding the complete NNLO soft-plus-virtual corrections to the exact NLO QCD result. The aN<sup>3</sup>LO predictions are derived by further adding the complete N<sup>3</sup>LO soft-gluon corrections to the aNNLO results.

The paper is organized as follows. In Section 2, we describe the soft-gluon resummation formalism for  $\gamma W$  partonic processes and present detailed analytical results for the soft-gluon corrections through N<sup>3</sup>LO. In Section 3, we present numerical results for the total cross section through aN<sup>3</sup>LO

at 13 TeV and 13.6 TeV collision energies at the LHC. We provide separate results for  $\gamma W^+$  and  $\gamma W^-$  production and give uncertainties from scale variation and from parton distributions. In Section 4, we present results for the photon differential distributions in transverse momentum at 13 and 13.6 TeV LHC energies. We conclude in Section 5.

## 2 Soft-gluon corrections for $\gamma W$ production

In this section, we discuss the resummation formalism that we use for the calculation of soft-gluon corrections in  $\gamma W$  production. The origin of the soft-gluon corrections is from the emission of soft (low-energy) gluons, which result in partial cancellations of infrared divergences between real-emission and virtual diagrams close to partonic threshold for the production of a  $\gamma W$  pair.

In this work we consider  $\gamma W$  production in proton-proton collisions, which occurs at leading-order through the following partonic processes

$$q(p_a) + \bar{q}'(p_b) \rightarrow \gamma(p_1) + W(p_2), \quad (2.1)$$

where  $q$  and  $\bar{q}'$  are quarks and antiquarks in the protons, and  $W$  denotes either a  $W^+$  or a  $W^-$  boson. We work in single-particle-inclusive kinematics where the photon is the observed particle. We define  $s = (p_a + p_b)^2$ ,  $t = (p_a - p_1)^2$ ,  $t_1 = t - m_W^2$ ,  $u = (p_b - p_1)^2$ ,  $u_1 = u - m_W^2$ , as well as a partonic threshold variable  $s_4 = (p_2 + p_g)^2 - m_W^2 = s + t + u - m_W^2$ , with  $m_W$  the  $W$ -boson mass and  $p_g$  the momentum of an additional gluon in the final state. Near partonic threshold  $p_g \rightarrow 0$  and, thus,  $s_4 \rightarrow 0$ . The soft-gluon corrections appear in the perturbative series in the strong coupling,  $\alpha_s$ , as logarithms of  $s_4$ , i.e.  $[(\ln^k(s_4/m_W^2))/s_4]_+$ , with  $0 \leq k \leq 2n - 1$  at  $n$ th order in  $\alpha_s$ .

The resummation of soft-gluon corrections follows as a consequence of the factorization properties of the (differential) cross section under Laplace transforms. We express the differential hadronic cross section,  $d\sigma_{pp \rightarrow \gamma W}$ , as a convolution in the form

$$d\sigma_{pp \rightarrow \gamma W} = \sum_{q, \bar{q}'} \int dx_a dx_b \phi_{q/p}(x_a, \mu_F) \phi_{\bar{q}'/p}(x_b, \mu_F) d\hat{\sigma}_{q\bar{q}' \rightarrow \gamma W}(s_4, \mu_F), \quad (2.2)$$

where  $d\hat{\sigma}_{q\bar{q}' \rightarrow \gamma W}$  is the differential partonic cross section at factorization scale  $\mu_F$ , while  $\phi_{q/p}$  and  $\phi_{\bar{q}'/p}$  are parton distribution functions (pdf) with  $x_a, x_b$  the momentum fractions of partons  $q, \bar{q}'$  in the two protons.

The LO differential partonic cross section is given by

$$\frac{d\hat{\sigma}_{q\bar{q}' \rightarrow \gamma W}^{(0)}}{dt_1 du_1} = F_{q\bar{q}' \rightarrow \gamma W}^{(0)} \delta(s_4) \quad (2.3)$$

where

$$F_{q\bar{q}' \rightarrow \gamma W}^{(0)} = \frac{\alpha^2 \pi m_Z^2}{54 s^2 (m_Z^2 - m_W^2)} \frac{(t - 2u)^2 (m_W^4 + s^2 - 2tu)}{(s - m_W^2)^2 t u} \quad (2.4)$$

with  $\alpha$  the electromagnetic coupling and  $m_Z$  the  $Z$ -boson mass.

The resummed cross section is given under Laplace transforms, with  $N$  the transform variable, by

$$\begin{aligned} d\hat{\sigma}_{q\bar{q}' \rightarrow \gamma W}^{res}(N) &= \exp[E_q(N_a) + E_{\bar{q}'}(N_b)] \exp \left[ 2 \int_{\mu_F}^{\sqrt{s}} \frac{d\mu}{\mu} \left( \gamma_{q/q}(\tilde{N}_a, \alpha_s(\mu)) + \gamma_{\bar{q}'/\bar{q}'}(\tilde{N}_b, \alpha_s(\mu)) \right) \right] \\ &\times H_{q\bar{q}' \rightarrow \gamma W}(\alpha_s(\sqrt{s})) \tilde{S}_{q\bar{q}' \rightarrow \gamma W}(\alpha_s(\sqrt{s}/N)). \end{aligned} \quad (2.5)$$

In the first exponent of Eq. (2.5),

$$E_q(N_a) = \int_0^1 dz \frac{z^{N_a-1} - 1}{1-z} \left\{ \int_1^{(1-z)^2} \frac{d\lambda}{\lambda} A_q(\alpha_s(\lambda s)) + D_q[\alpha_s((1-z)^2 s)] \right\} \quad (2.6)$$

with  $N_a = N(-u_1/s)$ , and a similar expression holds for  $E_{\bar{q}}(N_b)$  with  $N_b = N(-t_1/s)$ . The first integrand in Eq. (2.6) admits the perturbative expansion  $A_q = \sum_{n=1}^{\infty} (\alpha_s/\pi)^n A_q^{(n)}$ . The first term in this expansion is  $A_q^{(1)} = C_F = (N_c^2 - 1)/(2N_c)$  [27], where  $N_c = 3$  is the number of colors. The second term,  $A_q^{(2)}$ , is given by [28]

$$A_q^{(2)} = C_F C_A \left( \frac{67}{36} - \frac{\zeta_2}{2} \right) - \frac{5}{18} C_F n_f, \quad (2.7)$$

where  $\zeta_2 = \pi^2/6$ ,  $C_A = N_c$ , and  $n_f = 5$  is the number of light-quark flavors. Finally, the third term  $A_q^{(3)}$  is given by [40]

$$\begin{aligned} A_q^{(3)} = & C_F C_A^2 \left( \frac{245}{96} - \frac{67}{36} \zeta_2 + \frac{11}{24} \zeta_3 + \frac{11}{8} \zeta_4 \right) + C_F^2 n_f \left( -\frac{55}{96} + \frac{\zeta_3}{2} \right) \\ & + C_F C_A n_f \left( -\frac{209}{432} + \frac{5}{18} \zeta_2 - \frac{7}{12} \zeta_3 \right) - C_F \frac{n_f^2}{108} \end{aligned} \quad (2.8)$$

where  $\zeta_3 = 1.202056903 \dots$  and  $\zeta_4 = \pi^4/90$ . The second integrand in Eq. (2.6) has the perturbative expansion  $D_q = \sum_{n=1}^{\infty} (\alpha_s/\pi)^n D_q^{(n)}$ . In the Feynman gauge, the one-loop term  $D_q^{(1)} = 0$ , while at two loops [41]

$$D_q^{(2)} = C_F C_A \left( -\frac{101}{54} + \frac{11}{6} \zeta_2 + \frac{7}{4} \zeta_3 \right) + C_F n_f \left( \frac{7}{27} - \frac{\zeta_2}{3} \right), \quad (2.9)$$

and at three loops [42]

$$\begin{aligned} D_q^{(3)} = & C_F C_A^2 \left( -\frac{297029}{46656} + \frac{6139}{648} \zeta_2 + \frac{2509}{216} \zeta_3 - \frac{187}{48} \zeta_4 - \frac{11}{12} \zeta_2 \zeta_3 - 3\zeta_5 \right) \\ & + C_F C_A n_f \left( \frac{31313}{23328} - \frac{1837}{648} \zeta_2 - \frac{155}{72} \zeta_3 + \frac{23}{24} \zeta_4 \right) \\ & + C_F^2 n_f \left( \frac{1711}{1728} - \frac{\zeta_2}{4} - \frac{19}{36} \zeta_3 - \frac{\zeta_4}{4} \right) + C_F n_f^2 \left( -\frac{29}{729} + \frac{5}{27} \zeta_2 + \frac{5}{54} \zeta_3 \right) \end{aligned} \quad (2.10)$$

where  $\zeta_5 = 1.036927755 \dots$ .

In the second exponent of Eq. (2.5), the quantity  $\gamma_{q/q}$  is the moment-space anomalous dimension of the  $\overline{\text{MS}}$  density  $\phi_{q/q}$  [43–47] (and similarly for  $\gamma_{\bar{q}/\bar{q}}$ ), and it can be expressed as  $\gamma_{q/q}(\tilde{N}) = -A_q \ln \tilde{N} + \gamma_q$  where  $\tilde{N} = N e^{\gamma_E}$  with  $\gamma_E$  the Euler constant. The perturbative expansion of the parton anomalous dimension is  $\gamma_q = \sum_{n=1}^{\infty} (\alpha_s/\pi)^n \gamma_q^{(n)}$  with  $\gamma_q^{(1)} = 3C_F/4$  and

$$\gamma_q^{(2)} = C_F^2 \left( \frac{3}{32} - \frac{3}{4} \zeta_2 + \frac{3}{2} \zeta_3 \right) + C_F C_A \left( \frac{17}{96} + \frac{11}{12} \zeta_2 - \frac{3}{4} \zeta_3 \right) - C_F n_f \left( \frac{1}{48} + \frac{\zeta_2}{6} \right). \quad (2.11)$$

We expand Eq. (2.5) to fixed order and then invert back to momentum space to derive results for the physical cross section. We further define

$$\mathcal{D}_k(s_4) = \left[ \frac{\ln^k(s_4/m_W^2)}{s_4} \right]_+. \quad (2.12)$$

The NLO soft-plus-virtual ( $S + V$ ) corrections to the partonic cross section are given by

$$\frac{d\hat{\sigma}_{q\bar{q}' \rightarrow \gamma W}^{(1)S+V}}{dt_1 du_1} = F_{q\bar{q}' \rightarrow \gamma W}^{(0)} \frac{\alpha_s(\mu_R)}{\pi} \{c_3 \mathcal{D}_1(s_4) + c_2 \mathcal{D}_0(s_4) + c_1 \delta(s_4)\} \quad (2.13)$$

where  $\mu_R$  is the renormalization scale,  $c_3 = 4C_F$ ,

$$c_2 = -2C_F \ln\left(\frac{t_1 u_1}{m_W^4}\right) - 2C_F \ln\left(\frac{\mu_F^2}{s}\right), \quad (2.14)$$

and

$$c_1 = C_F \ln^2\left(\frac{-t_1}{m_W^2}\right) + C_F \ln^2\left(\frac{-u_1}{m_W^2}\right) + \left[C_F \ln\left(\frac{t_1 u_1}{m_W^4}\right) - 2\gamma_q^{(1)}\right] \ln\left(\frac{\mu_F^2}{s}\right) + V_1, \quad (2.15)$$

where  $V_1 = 2C_F(-2 + \zeta_2)$  denotes the contribution of the one-loop virtual corrections [48–50].

The NNLO soft-plus-virtual corrections are given by

$$\frac{d\hat{\sigma}_{q\bar{q}' \rightarrow \gamma W}^{(2)S+V}}{dt_1 du_1} = F_{q\bar{q}' \rightarrow \gamma W}^{(0)} \frac{\alpha_s^2(\mu_R)}{\pi^2} \left\{ \sum_{k=0}^3 C_k^{(2)} D_k(s_4) + C_\delta^{(2)} \delta(s_4) \right\} \quad (2.16)$$

where

$$\begin{aligned} C_3^{(2)} &= \frac{1}{2}c_3^2, \\ C_2^{(2)} &= \frac{3}{2}c_3c_2 - \frac{\beta_0}{4}c_3, \\ C_1^{(2)} &= c_3c_1 + c_2^2 - \zeta_2c_3^2 - \frac{\beta_0}{2}c_2 + 4A_q^{(2)} - \beta_0C_F \ln\left(\frac{\mu_F^2}{\mu_R^2}\right), \\ C_0^{(2)} &= c_2c_1 - \zeta_2c_3c_2 + \zeta_3c_3^2 + 2D_q^{(2)} - \frac{\beta_0}{2}C_F \left[ \ln^2\left(\frac{-t_1}{m_W^2}\right) + \ln^2\left(\frac{-u_1}{m_W^2}\right) \right] \\ &\quad - 2A_q^{(2)} \ln\left(\frac{t_1 u_1}{m_W^4}\right) + \frac{\beta_0}{4}c_2 \ln\left(\frac{\mu_R^2}{s}\right) - 2A_q^{(2)} \ln\left(\frac{\mu_F^2}{s}\right) + \frac{\beta_0}{4}C_F \ln^2\left(\frac{\mu_F^2}{s}\right), \\ C_\delta^{(2)} &= V_2 + \frac{1}{2}(c_1^2 - V_1^2) - \frac{\zeta_2}{2}c_2^2 + \zeta_3c_3c_2 + \frac{\beta_0}{6}C_F \left[ \ln^3\left(\frac{-t_1}{m_W^2}\right) + \ln^3\left(\frac{-u_1}{m_W^2}\right) \right] \\ &\quad + \left(\frac{\beta_0}{4}C_F + A_q^{(2)}\right) \left[ \ln^2\left(\frac{-t_1}{m_W^2}\right) + \ln^2\left(\frac{-u_1}{m_W^2}\right) \right] + \frac{\beta_0}{4}c_1 \ln\left(\frac{\mu_R^2}{s}\right) - 2\gamma_q^{(2)} \ln\left(\frac{\mu_F^2}{s}\right) \\ &\quad + A_q^{(2)} \ln\left(\frac{t_1 u_1}{m_W^4}\right) \ln\left(\frac{\mu_F^2}{s}\right) + \frac{\beta_0}{8} \left[ 2\gamma_q^{(1)} - C_F \ln\left(\frac{t_1 u_1}{m_W^4}\right) \right] \ln^2\left(\frac{\mu_F^2}{s}\right), \end{aligned} \quad (2.17)$$

with  $\beta_0 = 11C_A/3 - 2n_f/3$  denoting the lowest-order  $\beta$  function [51–53] and

$$\begin{aligned} V_2 &= C_F^2 \left( \frac{511}{64} - \frac{35}{8}\zeta_2 - \frac{15}{4}\zeta_3 + \frac{\zeta_2^2}{10} \right) + C_F C_A \left( -\frac{1535}{192} + \frac{37}{9}\zeta_2 + \frac{7}{4}\zeta_3 - \frac{3}{20}\zeta_2^2 \right) \\ &\quad + C_F n_f \left( \frac{127}{96} - \frac{7}{9}\zeta_2 + \frac{\zeta_3}{2} \right) \end{aligned} \quad (2.18)$$

denoting the contribution of the virtual two-loop corrections [54].

The N<sup>3</sup>LO soft-gluon ( $S$ ) corrections are given by

$$\frac{d^2 \hat{\sigma}_{q\bar{q}' \rightarrow \gamma W}^{(3)S}}{dt_1 du_1} = F_{q\bar{q}' \rightarrow \gamma W}^{(0)} \frac{\alpha_s^3(\mu_R)}{\pi^3} \sum_{k=0}^5 C_k^{(3)} D_k(s_4) \quad (2.19)$$

where

$$\begin{aligned} C_5^{(3)} &= \frac{1}{8} c_3^3, \\ C_4^{(3)} &= \frac{5}{8} c_3^2 c_2 - \frac{5}{24} c_3^2 \beta_0, \\ C_3^{(3)} &= c_3 c_2^2 + \frac{1}{2} c_3^2 c_1 - \zeta_2 c_3^3 + \frac{\beta_0^2}{12} c_3 - \frac{5}{6} \beta_0 c_3 c_2 + 4 c_3 A_q^{(2)} - \beta_0 C_F c_3 \ln \left( \frac{\mu_F^2}{\mu_R^2} \right), \\ C_2^{(3)} &= \frac{3}{2} c_3 c_2 c_1 + \frac{1}{2} c_2^3 - 3 \zeta_2 c_3^2 c_2 + \frac{5}{2} \zeta_3 c_3^3 - \frac{\beta_0}{4} c_3 c_1 + \frac{9}{8} \beta_0 \zeta_2 c_3^2 - C_F \frac{\beta_1}{4} \\ &\quad + (3 c_2 - \beta_0) \left[ -\frac{\beta_0}{4} c_2 + 2 A_q^{(2)} - \frac{\beta_0}{2} C_F \ln \left( \frac{\mu_F^2}{\mu_R^2} \right) \right] - \frac{3}{2} c_3 X_1, \\ C_1^{(3)} &= \frac{1}{2} c_3 c_1^2 + c_2^2 c_1 - \zeta_2 c_3^2 c_1 - \frac{5}{2} \zeta_2 c_3 c_2^2 + 5 \zeta_3 c_3^2 c_2 + \frac{5}{4} \zeta_2^2 c_3^3 - \frac{15}{4} \zeta_4 c_3^3 \\ &\quad - \frac{\beta_0^2}{4} \zeta_2 c_3 - \frac{5}{3} \beta_0 \zeta_3 c_3^2 + \beta_0 \zeta_2 c_3 c_2 + 4 A_q^{(3)} + C_F \frac{\beta_1}{4} \ln \left( \frac{t_1 u_1}{m_W^4} \right) \\ &\quad + (2 c_1 - 5 \zeta_2 c_3) \left[ -\frac{\beta_0}{4} c_2 + 2 A_q^{(2)} - \frac{\beta_0}{2} C_F \ln \left( \frac{\mu_F^2}{\mu_R^2} \right) \right] + C_F \frac{\beta_1}{4} \ln \left( \frac{\mu_R^2}{s} \right) \\ &\quad - 2 \beta_0 A_q^{(2)} \ln \left( \frac{\mu_F^2}{\mu_R^2} \right) + C_F \frac{\beta_0^2}{4} \ln^2 \left( \frac{\mu_F^2}{\mu_R^2} \right) + (\beta_0 - 2 c_2) X_1 + c_3 X_0, \\ C_0^{(3)} &= \frac{1}{2} c_2 c_1^2 + 3 \zeta_5 c_3^3 - \frac{15}{4} \zeta_4 c_3^2 c_2 - 2 \zeta_2 \zeta_3 c_3^3 + \zeta_3 c_3^2 c_1 + 2 \zeta_3 c_3 c_2^2 + \frac{5}{4} \zeta_2^2 c_3^2 c_2 - \zeta_2 c_3 c_2 c_1 - \frac{\zeta_2}{2} c_2^3 \\ &\quad + \frac{\beta_0}{12} c_3 (15 \zeta_4 c_3 - 8 \zeta_3 c_2 - 6 \zeta_2^2 c_3 + 3 \zeta_2 c_1) + 2 D_q^{(3)} - \frac{C_F}{6} \beta_0^2 \left[ \ln^3 \left( \frac{-t_1}{m_W^2} \right) + \ln^3 \left( \frac{-u_1}{m_W^2} \right) \right] \\ &\quad - \left[ \frac{\beta_0}{4} (C_F \beta_0 + 4 A_q^{(2)}) + \frac{\beta_1}{8} C_F \right] \left[ \ln^2 \left( \frac{-t_1}{m_W^2} \right) + \ln^2 \left( \frac{-u_1}{m_W^2} \right) \right] \\ &\quad + (\beta_0 D_q^{(2)} - 2 A_q^{(3)}) \ln \left( \frac{t_1 u_1}{m_W^4} \right) + (4 \zeta_3 c_3 - 3 \zeta_2 c_2) \left[ -\frac{\beta_0}{4} c_2 + 2 A_q^{(2)} - \frac{\beta_0}{2} C_F \ln \left( \frac{\mu_F^2}{\mu_R^2} \right) \right] \\ &\quad + D_q^{(2)} \beta_0 \ln \left( \frac{\mu_R^2}{s} \right) - 2 A_q^{(3)} \ln \left( \frac{\mu_F^2}{s} \right) - \frac{\beta_0^2}{4} C_F \left[ \ln^2 \left( \frac{-t_1}{m_W^2} \right) + \ln^2 \left( \frac{-u_1}{m_W^2} \right) \right] \ln \left( \frac{\mu_R^2}{s} \right) \\ &\quad - \left( A_q^{(2)} \beta_0 + C_F \frac{\beta_1}{8} \right) \ln \left( \frac{t_1 u_1}{m_W^4} \right) \ln \left( \frac{\mu_R^2}{s} \right) + \frac{\beta_0^2}{16} c_2 \ln^2 \left( \frac{\mu_R^2}{s} \right) + \frac{\beta_0^2}{8} C_F \ln^2 \left( \frac{\mu_F^2}{s} \right) \ln \left( \frac{\mu_R^2}{s} \right) \\ &\quad + \frac{1}{16} (C_F \beta_1 + 8 \beta_0 A_q^{(2)}) \left[ \ln^2 \left( \frac{\mu_F^2}{\mu_R^2} \right) - \ln^2 \left( \frac{\mu_R^2}{s} \right) \right] - C_F \frac{\beta_0^2}{24} \ln^3 \left( \frac{\mu_F^2}{s} \right) \\ &\quad + (\zeta_2 c_3 - c_1) X_1 + c_2 X_0, \end{aligned} \quad (2.20)$$

with

$$\begin{aligned} X_1 &= \frac{\beta_0}{4} \zeta_2 c_3 - 2 D_q^{(2)} + \frac{\beta_0}{2} C_F \left[ \ln^2 \left( \frac{-t_1}{m_W^2} \right) + \ln^2 \left( \frac{-u_1}{m_W^2} \right) \right] + 2 A_q^{(2)} \ln \left( \frac{t_1 u_1}{m_W^4} \right) \\ &\quad - \frac{\beta_0}{4} c_2 \ln \left( \frac{\mu_R^2}{s} \right) + 2 A_q^{(2)} \ln \left( \frac{\mu_F^2}{s} \right) - \frac{\beta_0}{4} C_F \ln^2 \left( \frac{\mu_F^2}{s} \right), \end{aligned} \quad (2.21)$$

$$\begin{aligned}
X_0 = & V_2 - \frac{1}{2}V_1^2 + \frac{1}{20}\zeta_2^2 c_3^2 + \frac{\beta_0}{6}\zeta_3 c_3 - \frac{\beta_0}{4}\zeta_2 c_2 + 2A_q^{(2)}\zeta_2 + \frac{\beta_0}{6}C_F \left[ \ln^3 \left( \frac{-t_1}{m_W^2} \right) + \ln^3 \left( \frac{-u_1}{m_W^2} \right) \right] \\
& + \left( C_F \frac{\beta_0}{4} + A_q^{(2)} \right) \left[ \ln^2 \left( \frac{-t_1}{m_W^2} \right) + \ln^2 \left( \frac{-u_1}{m_W^2} \right) \right] + \frac{\beta_0}{4}c_1 \ln \left( \frac{\mu_R^2}{s} \right) - \frac{\beta_0}{2}\zeta_2 C_F \ln \left( \frac{\mu_F^2}{\mu_R^2} \right) \\
& + \left[ -2\gamma_q^{(2)} + A_q^{(2)} \ln \left( \frac{t_1 u_1}{m_W^4} \right) \right] \ln \left( \frac{\mu_F^2}{s} \right) + \frac{\beta_0}{8} \left[ 2\gamma_q^{(1)} - C_F \ln \left( \frac{t_1 u_1}{m_W^4} \right) \right] \ln^2 \left( \frac{\mu_F^2}{s} \right), \quad (2.22)
\end{aligned}$$

and  $\beta_1 = 34C_A^2/3 - 2C_F n_f - 10C_A n_f/3$  [55–57] denoting the coefficient of the second term in the perturbative expansion of the  $\beta$  function.

### 3 Total cross sections for $\gamma W^+$ and $\gamma W^-$ at 13 and 13.6 TeV

In this section we present results for  $\gamma W$  production at the LHC, for two center-of-mass energies, namely 13 TeV and 13.6 TeV. We present separate results for  $\gamma W^+$  and  $\gamma W^-$  total cross sections. The complete NLO results (including QCD and electroweak corrections) are calculated using MADGRAPH5\_AMC@NLO [58, 59]. We use MSHT20 nnlo [60] and an<sup>3</sup>lo pdf [61] in our calculations (we use lower-case letters for the order of the pdf, and capital letters for the order of the calculation of the perturbative cross section, in order to avoid confusion). We take  $m_W = 80.3692$  GeV,  $m_Z = 91.188$  GeV [62], and  $\alpha^{-1} = 127.9$ . The central results are obtained by setting  $\mu_F = \mu_R = m_W$ . To obtain scale uncertainties, we vary the factorization and renormalization scales independently from each other over the range  $m_W/2$  to  $2m_W$ , and we also compute pdf uncertainties. The aNNLO cross sections are calculated by adding second-order soft-plus-virtual QCD corrections to the complete NLO result. Third-order soft-gluon corrections are further added in order to derive a result at aN<sup>3</sup>LO.

$pp \rightarrow \gamma W^+$ and $pp \rightarrow \gamma W^-$ cross sections at 13 TeV				$p_{\gamma T}^{\text{cut}} = 25$ GeV	
process	pdf order	$\sigma$ LO (pb)	$\sigma$ NLO (pb)	$\sigma$ aNNLO (pb)	$\sigma$ aN <sup>3</sup> LO (pb)
$\gamma W^+$	nnlo	$23.6^{+1.7+0.4}_{-1.9-0.3}$	$55.3^{+5.2+0.5}_{-5.1-0.6}$	$60.4^{+4.6+0.5}_{-5.6-0.7}$	$62.0^{+5.1+0.5}_{-5.9-0.7}$
$\gamma W^+$	an <sup>3</sup> lo	$23.8^{+1.6+0.4}_{-1.8-0.3}$	$55.2^{+5.1+0.6}_{-5.0-0.6}$	$60.3^{+4.5+0.7}_{-5.5-0.7}$	$61.9^{+5.0+0.7}_{-5.8-0.7}$
$\gamma W^-$	nnlo	$16.1^{+1.2+0.3}_{-1.3-0.2}$	$42.1^{+4.3+0.5}_{-4.1-0.5}$	$45.4^{+4.0+0.5}_{-4.5-0.6}$	$46.5^{+4.3+0.5}_{-4.8-0.6}$
$\gamma W^-$	an <sup>3</sup> lo	$16.2^{+1.2+0.3}_{-1.3-0.2}$	$42.0^{+4.2+0.4}_{-4.1-0.6}$	$45.3^{+3.9+0.5}_{-4.5-0.5}$	$46.4^{+4.2+0.5}_{-4.7-0.6}$

Table 1:  $pp \rightarrow \gamma W^+$  and  $pp \rightarrow \gamma W^-$  cross sections at the LHC with  $\sqrt{S} = 13$  TeV and MSHT20 pdf. The central results are for  $\mu_F = \mu_R = m_W$  and are shown together with scale and pdf uncertainties.

In Table 1, we present the cross sections for  $\gamma W^+$  and  $\gamma W^-$  production at 13 TeV LHC energy with a cut of 25 GeV on the transverse momentum,  $p_T$ , of the photon. Results are given at LO, NLO, aNNLO, and aN<sup>3</sup>LO with scale and pdf uncertainties using MSHT20 nnlo and an<sup>3</sup>lo pdf. We note that at LO there is no  $\mu_R$  uncertainty since that order is  $\alpha_s^0$ . The magnitude of the scale uncertainty with independent variation of  $\mu_F$  and  $\mu_R$  is somewhat larger at NLO than at LO; while at aNNLO and aN<sup>3</sup>LO it is similar to the one at NLO. On the other hand, we note that if we vary the factorization and renormalization scales simultaneously, then the scale uncertainty, at the same perturbative order, is much smaller and is reduced when going to higher orders. For example, at 13 TeV using nnlo pdf for the  $\gamma W^+$  cross section with scale uncertainties from simultaneous variation of  $\mu_F$  and  $\mu_R$ , we find  $55.3^{+1.7}_{-1.6}$  at NLO,  $60.4^{+1.6}_{-1.5}$  at aNNLO, and  $62.0^{+0.8}_{-0.2}$  at aN<sup>3</sup>LO, i.e we see progressively smaller uncertainties at higher orders; the corresponding values for the  $\gamma W^-$

cross section are  $42.1^{+1.5}_{-1.3}$ ,  $45.4^{+1.3}_{-1.1}$ , and  $46.5^{+0.7}_{-0.0}$  where again the aN<sup>3</sup>LO uncertainty is smaller than at aNNLO which in turn is smaller than at NLO.

$pp \rightarrow \gamma W^+$ and $pp \rightarrow \gamma W^-$ cross sections at 13.6 TeV $p_{\gamma T}^{\text{cut}} = 25$ GeV					
process	pdf order	$\sigma$ LO (pb)	$\sigma$ NLO (pb)	$\sigma$ aNNLO (pb)	$\sigma$ aN <sup>3</sup> LO (pb)
$\gamma W^+$	nnlo	$24.8^{+1.8+0.4}_{-2.0-0.3}$	$58.6^{+5.7+0.5}_{-5.5-0.6}$	$63.9^{+5.1+0.5}_{-6.0-0.7}$	$65.6^{+5.6+0.6}_{-6.3-0.7}$
$\gamma W^+$	an <sup>3</sup> lo	$25.1^{+1.7+0.3}_{-2.1-0.4}$	$58.5^{+5.6+0.7}_{-5.5-0.7}$	$63.8^{+5.0+0.7}_{-5.9-0.7}$	$65.5^{+5.6+0.8}_{-6.2-0.7}$
$\gamma W^-$	nnlo	$17.1^{+1.2+0.2}_{-1.5-0.3}$	$44.9^{+4.6+0.4}_{-4.5-0.6}$	$48.4^{+4.3+0.5}_{-4.9-0.6}$	$49.5^{+4.7+0.5}_{-5.2-0.6}$
$\gamma W^-$	an <sup>3</sup> lo	$17.2^{+1.2+0.2}_{-1.5-0.3}$	$44.7^{+4.6+0.5}_{-4.4-0.5}$	$48.2^{+4.3+0.6}_{-4.8-0.6}$	$49.3^{+4.7+0.6}_{-5.0-0.6}$

Table 2:  $pp \rightarrow \gamma W^+$  and  $pp \rightarrow \gamma W^-$  cross sections at the LHC with  $\sqrt{S} = 13.6$  TeV and MSHT20 pdf. The central results are for  $\mu_F = \mu_R = m_W$  and are shown together with scale and pdf uncertainties.

In Table 2, we present the cross sections at LO, NLO, aNNLO, and aN<sup>3</sup>LO (with scale and pdf uncertainties) for  $\gamma W^+$  and  $\gamma W^-$  production at 13.6 TeV LHC energy, again with a cut of 25 GeV on the  $p_T$  of the photon and using MSHT20 nnlo and an<sup>3</sup>lo pdf. Here the behavior of the scale uncertainties is similar to what was discussed before for the 13 TeV case.

As can be seen from both Tables, the enhancement from the aNNLO and aN<sup>3</sup>LO contributions is significant. We also note that the NNLO  $\delta(s_4)$  terms (which include the virtual corrections) are small compared to the NNLO soft-gluon corrections; their contribution to the total NNLO soft+virtual corrections is less than 20% at both 13 and 13.6 TeV energies.

Next, we consider the decay of the  $W$  boson into charged leptons and neutrinos. We use MATRIX [63] to compute the cross section for  $pp \rightarrow e^- \bar{\nu}_e \gamma$  and  $pp \rightarrow e^+ \nu_e \gamma$  at 13 TeV, including QCD corrections up to NNLO and using MSHT20 nnlo pdf. The cross section is computed in the  $G_\mu$ -scheme, where the electromagnetic coupling associated with the emission of an on-shell photon is taken to be  $\alpha = 1/137.036$ , while the other electromagnetic couplings are equal to the one defined in terms of the Fermi constant  $G_\mu$ , namely  $\alpha = \sqrt{2} G_\mu m_W^2 (1 - m_W^2/m_Z^2)/\pi$ . As input parameters we use  $m_W = 80.3692$  GeV,  $m_Z = 91.188$  GeV,  $G_\mu = 1.16638 \times 10^{-5}$  GeV<sup>-2</sup> [62]. Furthermore, the cross section is computed applying some fiducial cuts inspired by a recent experimental analysis [14], namely  $p_{eT} > 25$  GeV,  $|\eta_e| < 2.5$ ,  $p_{\gamma T} > 25$  GeV,  $|\eta_\gamma| < 2.5$  and  $\Delta R(e, \gamma) > 0.5$ . Here  $\Delta R = \sqrt{\Delta\varphi^2 + \Delta\eta^2}$ , where  $\Delta\varphi$  and  $\Delta\eta$  are the spatial separations in azimuthal angle  $\varphi$  and pseudorapidity  $\eta$  between the lepton and photon. The central results are obtained by setting  $\mu_F = \mu_R = m_W$ , while the scale uncertainties are obtained by varying the factorization and renormalization scales independently. For the process  $pp \rightarrow e^- \bar{\nu}_e \gamma$  we find  $0.829^{+0.075}_{-0.085}$  pb at LO,  $2.39^{+0.26}_{-0.25}$  pb at NLO, and  $2.93^{+0.14}_{-0.16}$  pb at NNLO (for simultaneous variation of  $\mu_F$  and  $\mu_R$ , we find  $2.39^{+0.08}_{-0.08}$  pb at NLO and  $2.93^{+0.12}_{-0.09}$  pb at NNLO). These results show a NLO/LO  $K$ -factor equal to 2.88 and a NNLO/NLO  $K$ -factor equal to 1.23. For  $pp \rightarrow e^+ \nu_e \gamma$  at 13 TeV we find  $1.03^{+0.09}_{-0.10}$  pb at LO,  $2.75^{+0.28}_{-0.28}$  pb at NLO, and  $3.34^{+0.14}_{-0.18}$  pb at NNLO (for simultaneous  $\mu_F$  and  $\mu_R$  variation, we find  $2.75^{+0.09}_{-0.09}$  pb at NLO and  $3.34^{+0.12}_{-0.10}$  pb at NNLO). For this process we have a NLO/LO  $K$ -factor equal to 2.67 and a NNLO/NLO  $K$ -factor equal to 1.21. We note that the  $K$ -factors for the processes with decays and the selected cuts are significantly bigger than for those without decays. Assuming that the aN<sup>3</sup>LO  $K$ -factors are also bigger for the decay processes, we would infer a minimum value for the aN<sup>3</sup>LO cross section at 13 TeV of 3.00 pb for  $pp \rightarrow e^- \bar{\nu}_e \gamma$  and of 3.43 pb for  $pp \rightarrow e^+ \nu_e \gamma$ . However, since we cannot implement the cuts on the decay particles in our formalism, we cannot make more predictions than this minimum value for the aN<sup>3</sup>LO cross section.

## 4 Photon $p_T$ distributions at 13 and 13.6 TeV

In this section we present results for the photon transverse-momentum differential distributions in  $\gamma W^+$  and  $\gamma W^-$  production at the LHC. As for the total cross section, we take  $m_W = 80.3692$  GeV,  $m_Z = 91.188$  GeV, and  $\alpha^{-1} = 127.9$ . Here we use  $\text{an}^3\text{lo}$  pdf and present the central results which are obtained by setting  $\mu_F = \mu_R = m_W$ . Again, the  $\text{aN}^2\text{LO}$  results are obtained by adding second-order soft-plus-virtual QCD corrections to the complete NLO result. Third-order soft-gluon corrections are further added in order to derive a result at  $\text{aN}^3\text{LO}$ .

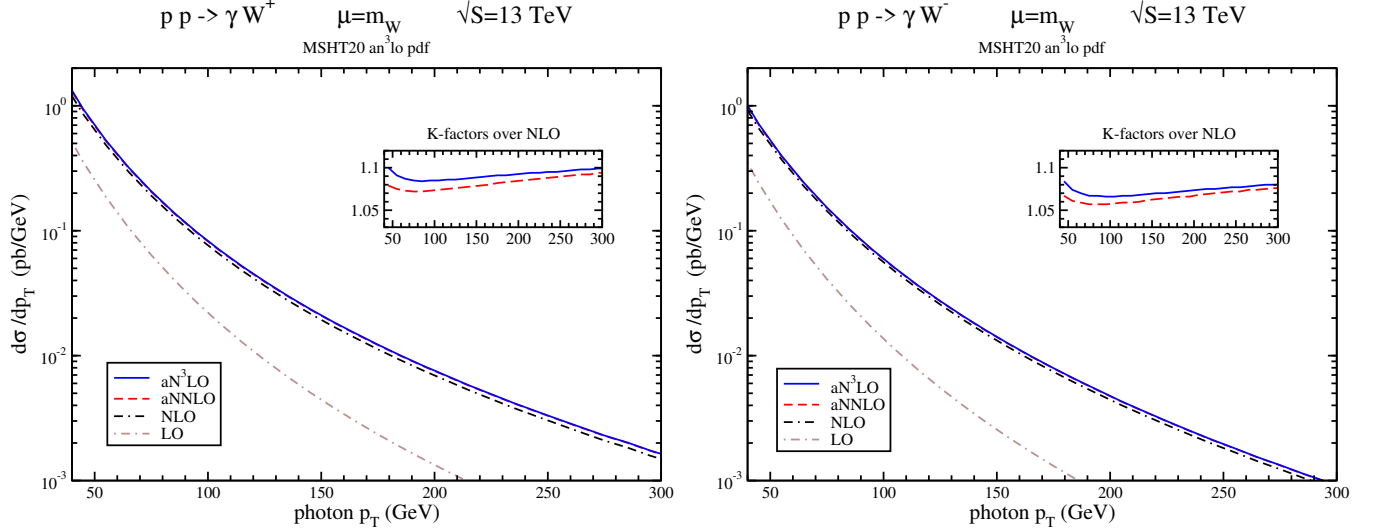


Figure 1: The photon  $p_T$  distributions through  $\text{aN}^3\text{LO}$  in  $\gamma W^+$  (left) and  $\gamma W^-$  (right) production in  $pp$  collisions at an LHC energy of 13 TeV. The inset plots display the  $K$ -factors relative to NLO.

In Fig. 1, we show the photon  $p_T$  distribution in  $\gamma W^+$  and  $\gamma W^-$  production at 13 TeV LHC energy through  $\text{aN}^3\text{LO}$ . The distributions fall quickly by several orders of magnitude as the photon transverse momentum increases. The inset plots show the  $K$ -factors, i.e. the ratios of the  $\text{aN}^2\text{LO}$  and  $\text{aN}^3\text{LO}$  distributions to NLO. The  $\text{aN}^2\text{LO}$  and  $\text{aN}^3\text{LO}$  distributions are practically on top of each other in the main logarithmic plots, but the inset plots clearly show the additional  $\text{aN}^3\text{LO}$  contributions in the  $K$ -factors. The dependence of the  $K$ -factors on the photon transverse momentum is mild. The  $K$ -factors in both plots take values between 1.05 and 1.1 in the  $p_T$  range shown, depending on the process and the perturbative order, they have a minimum at a  $p_T$  value of around 80 GeV, and they increase slowly at higher  $p_T$  values.

In Fig. 2, we show the photon  $p_T$  distribution in  $\gamma W^+$  and  $\gamma W^-$  production at 13.6 TeV LHC energy through  $\text{aN}^3\text{LO}$ . Similarly to the 13 TeV case, we see that the distributions fall very quickly with increasing photon  $p_T$ . The inset plots show the  $\text{aN}^2\text{LO}$  and  $\text{aN}^3\text{LO}$   $K$ -factors relative to NLO. The  $K$ -factors at 13.6 TeV are slightly smaller than those at 13 TeV, but the dependence on the transverse momentum is, again, mild. Indeed, they also reach a minimum value at  $p_T$  of around 80 GeV, and then they slowly increase at higher  $p_T$ .

## 5 Conclusions

In this paper we have provided a study of higher-order QCD corrections to  $\gamma W$  production in proton-proton collisions at the LHC, considering a center-of-mass energy of 13 TeV and 13.6 TeV.



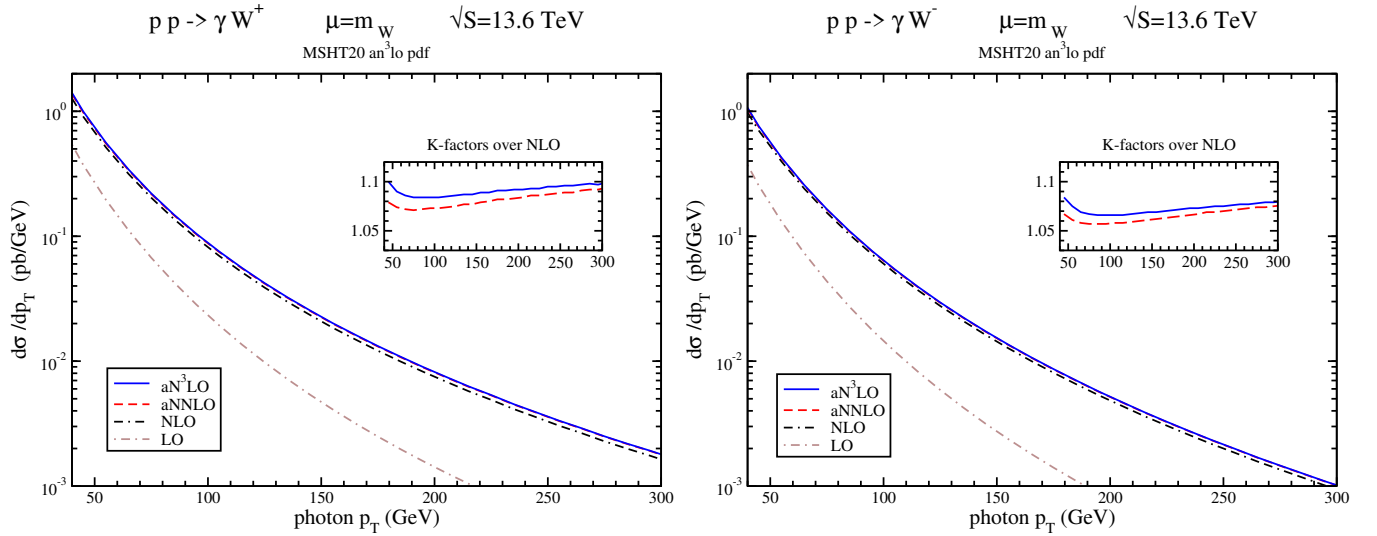


Figure 2: The photon  $p_T$  distributions through aN<sup>3</sup>LO in  $\gamma W^+$  (left) and  $\gamma W^-$  (right) production in  $pp$  collisions at an LHC energy of 13.6 TeV. The inset plots display the  $K$ -factors relative to NLO.

We have computed aNNLO QCD cross sections for both  $\gamma W^+$  and  $\gamma W^-$  production by adding the NNLO soft-plus-virtual QCD corrections to the complete NLO result. Our calculation showed that, at this order, soft-gluon corrections numerically dominate the virtual ones. Moreover, results at aN<sup>3</sup>LO have been derived by including third-order soft-gluon corrections. For the calculation of the total cross section, scale and pdf uncertainties have been also provided. From our results, we obtained that the relative uncertainties from factorization and renormalization scale variation do not change much at higher orders when performing an independent variation of the two scales over the range  $m_W/2$  to  $2m_W$ , while they decrease significantly when considering a simultaneous variation of these scales.

We have also computed aNNLO and aN<sup>3</sup>LO differential distributions in the transverse momentum of the photon at 13 and 13.6 TeV LHC energies, and we have presented separate results for the  $\gamma W^+$  and  $\gamma W^-$  processes. The distributions fall very quickly with increasing  $p_T$  of the photon; indeed, they decrease by several orders of magnitude over the  $p_T$  range in the plots. The  $K$ -factors relative to NLO show a mild dependence on the transverse momentum of the photon for both energies and processes, and they slowly increase at higher photon  $p_T$  values. Similarly to the total cross section, we find significant enhancements from the higher-order corrections.

This work is the first calculation of complete soft-gluon corrections at N<sup>3</sup>LO in single-particle-inclusive kinematics for a Standard Model process. Our results show that the enhancements to the total cross sections and the photon  $p_T$  distributions in  $\gamma W$  production at LHC energies from the inclusion of aNNLO and aN<sup>3</sup>LO contributions are significant.

## Acknowledgements

This material is based upon work supported by the National Science Foundation under Grant No. PHY 2412071.

# References

- [1] CDF Collaboration, *Measurement of  $W$ -photon couplings with CDF in  $p\bar{p}$  collisions at  $\sqrt{s} = 1.8$  TeV*, Phys. Rev. Lett. **74**, 1936 (1995).
- [2] D0 Collaboration, *Measurement of the  $WW\gamma$  gauge boson couplings in  $p\bar{p}$  collisions at  $\sqrt{s} = 1.8$  TeV*, Phys. Rev. Lett. **75**, 1034 (1995) [arXiv:hep-ex/9505007].
- [3] D0 Collaboration, *Limits on anomalous  $WW\gamma$  couplings from  $p\bar{p} \rightarrow W\gamma + X$  events at  $\sqrt{s} = 1.8$  TeV*, Phys. Rev. Lett. **78**, 3634 (1997) [arXiv:hep-ex/9612002].
- [4] CDF Collaboration, *Measurement of  $W\gamma$  and  $Z\gamma$  production in  $p\bar{p}$  collisions at  $\sqrt{s} = 1.96$  TeV*, Phys. Rev. Lett. **94**, 041803 (2005) [arXiv:hep-ex/0410008].
- [5] D0 Collaboration, *Measurement of the  $p\bar{p} \rightarrow W\gamma + X$  cross section at  $\sqrt{s} = 1.96$  TeV and  $WW\gamma$  anomalous coupling limits*, Phys. Rev. D **71**, 091108 (2005) [arXiv:hep-ex/0503048].
- [6] D0 Collaboration, *First study of the radiation-amplitude zero in  $W\gamma$  production and limits on anomalous  $WW\gamma$  couplings at  $\sqrt{s} = 1.96$  TeV*, Phys. Rev. Lett. **100**, 241805 (2008) [arXiv:0803.0030].
- [7] D0 Collaboration,  *$W\gamma$  production and limits on anomalous  $WW\gamma$  couplings in  $p\bar{p}$  collisions at  $\sqrt{s} = 1.96$  TeV*, Phys. Rev. Lett. **107**, 241803 (2011) [arXiv:1109.4432].
- [8] CMS Collaboration, *Measurement of  $W\gamma$  and  $Z\gamma$  production in  $pp$  collisions at  $\sqrt{s} = 7$  TeV*, Phys. Lett. B **701**, 535 (2011) [arXiv:1105.2758].
- [9] ATLAS Collaboration, *Measurement of  $W\gamma$  and  $Z\gamma$  production in proton-proton collisions at  $\sqrt{s} = 7$  TeV with the ATLAS detector*, JHEP **09**, 072 (2011) [arXiv:1106.1592].
- [10] ATLAS Collaboration, *Measurement of  $W\gamma$  and  $Z\gamma$  production cross sections in  $pp$  collisions at  $\sqrt{s} = 7$  TeV and limits on anomalous triple gauge couplings with the ATLAS detector*, Phys. Lett. B **717**, 49 (2012) [arXiv:1205.2531].
- [11] ATLAS Collaboration, *Measurement of  $W\gamma$  and  $Z\gamma$  production in  $pp$  collisions at  $\sqrt{s} = 7$  TeV with the ATLAS detector at the LHC*, Phys. Rev. D **87**, 112003 (2013) [Erratum: Phys. Rev. D **91**, 119901 (2015)] [arXiv:1302.1283].
- [12] CMS Collaboration, *Measurement of the  $W\gamma$  and  $Z\gamma$  inclusive cross sections in  $pp$  collisions at  $\sqrt{s} = 7$  TeV and limits on anomalous triple gauge boson couplings*, Phys. Rev. D **89**, 092005 (2014) [arXiv:1308.6832].
- [13] ATLAS Collaboration, *Search for new resonances in  $W\gamma$  and  $Z\gamma$  final states in  $pp$  collisions at  $\sqrt{s} = 8$  TeV with the ATLAS detector*, Phys. Lett. B **738**, 428 (2014) [arXiv:1407.8150].
- [14] CMS Collaboration, *Measurement of the  $W\gamma$  production cross section in proton-proton collisions at  $\sqrt{s} = 13$  TeV and constraints on effective field theory coefficients*, Phys. Rev. Lett. **126**, 252002 (2021) [arXiv:2102.02283].
- [15] CMS Collaboration, *Measurement of  $W^\pm\gamma$  differential cross sections in proton-proton collisions at  $\sqrt{s} = 13$  TeV and effective field theory constraints*, Phys. Rev. D **105**, 052003 (2022) [arXiv:2111.13948].

- [16] ATLAS Collaboration, *Search for high-mass  $W\gamma$  and  $Z\gamma$  resonances using hadronic  $W/Z$  boson decays from  $139\text{ fb}^{-1}$  of  $pp$  collisions at  $\sqrt{s} = 13\text{ TeV}$  with the ATLAS detector*, JHEP **07**, 125 (2023) [arXiv:2304.11962].
- [17] R.W. Brown, D. Sahdev, and K.O. Mikaelian,  *$W^\pm Z^0$  and  $W^\pm\gamma$  pair production in  $\nu e$ ,  $pp$ , and  $\bar{p}p$  collisions*, Phys. Rev. D **20**, 1164 (1979).
- [18] J. Smith, D. Thomas, and W. van Neerven, *QCD corrections to the reaction  $p+\bar{p} \rightarrow W+\gamma+X$* , Z. Phys. C **44**, 267 (1989).
- [19] S. Mendoza, J. Smith, and W. van Neerven, *Order- $\alpha_s^2$  QCD corrections to the reaction  $p+\bar{p} \rightarrow W^++\gamma+X$  in the soft-plus-virtual-gluon approximation*, Phys. Rev. D **47**, 3913 (1993).
- [20] L. Dixon, Z. Kunszt, and A. Signer, *Helicity amplitudes for  $\mathcal{O}(\alpha_s)$  production of  $W^+W^-$ ,  $W^\pm Z$ ,  $ZZ$ ,  $W^\pm\gamma$ , or  $Z\gamma$  pairs at hadron colliders*, Nucl. Phys. B **531**, 3 (1998) [arXiv:hep-ph/9803250].
- [21] E. Accomando, A. Denner, and S. Pozzorini, *Electroweak-correction effects in gauge-boson pair production at the CERN LHC*, Phys. Rev. D **65**, 073003 (2002) [arXiv:hep-ph/0110114].
- [22] K.L. Adamson, D. de Florian, and A. Signer, *Gluon induced contributions to  $WZ$  and  $W\gamma$  production at NNLO*, Phys. Rev. D **65**, 094041 (2002) [arXiv:hep-ph/0202132].
- [23] E. Accomando, A. Denner, and C. Meier, *Electroweak corrections to  $W\gamma$  and  $Z\gamma$  production at the LHC*, Eur. Phys. J. C **47**, 125 (2006) [arXiv:hep-ph/0509234].
- [24] J.M. Campbell, R.K. Ellis, and C. Williams, *Vector boson pair production at the LHC*, JHEP **07**, 018 (2011) [arXiv:1105.0020].
- [25] A. Denner, S. Dittmaier, M. Hecht, and C. Pasold *NLO QCD and electroweak corrections to  $W+\gamma$  production with leptonic  $W$ -boson decays*, JHEP **04**, 018 (2015) [arXiv:1412.7421].
- [26] M. Grazzini, S. Kallweit, and D. Rathlev,  *$W\gamma$  and  $Z\gamma$  production at the LHC in NNLO QCD*, JHEP **07**, 085 (2015) [arXiv:1504.01330].
- [27] G. Sterman, *Summation of large corrections to short-distance hadronic cross sections*, Nucl. Phys. B **281**, 310 (1987).
- [28] S. Catani and L. Trentadue, *Resummation of the QCD perturbative series for hard processes*, Nucl. Phys. B **327**, 323 (1989).
- [29] N. Kidonakis and G. Sterman, *Subleading logarithms in QCD hard scattering*, Phys. Lett. B **387**, 867 (1996).
- [30] N. Kidonakis and G. Sterman, *Resummation for QCD hard scattering*, Nucl. Phys. B **505**, 321 (1997) [arXiv:hep-ph/9705234].
- [31] E. Laenen, G. Oderda, and G. Sterman, *Resummation of threshold corrections for single-particle inclusive cross sections*, Phys. Lett. B **438**, 173 (1998) [arXiv:hep-ph/9806467].
- [32] N. Kidonakis and V. Del Duca, *Electroweak-boson hadroproduction at large transverse momentum: factorization, resummation, and NNLO corrections*, Phys. Lett. B **480**, 87 (2000) [arXiv:hep-ph/9911460].

- [33] N. Kidonakis and A. Sabio Vera, *W hadroproduction at large transverse momentum beyond next-to-leading order*, JHEP **02**, 027 (2004) [arXiv:hep-ph/0311266].
- [34] R.J. Gonsalves, N. Kidonakis, and A. Sabio Vera, *W production at large transverse momentum at the CERN Large Hadron Collider*, Phys. Rev. Lett. **95**, 222001 (2005) [arXiv:hep-ph/0507317].
- [35] N. Kidonakis, *Collinear and soft-gluon corrections to Higgs production at next-to-next-to-next-to-leading order*, Phys. Rev. D **77**, 053008 (2008) [arXiv:0711.0142].
- [36] N. Kidonakis, *Two-loop soft anomalous dimensions for single top quark associated production with a  $W^-$  or  $H^-$* , Phys. Rev. D **82**, 054018 (2010) [arXiv:1005.4451].
- [37] N. Kidonakis and R.J. Gonsalves, *Higher-order QCD corrections for the W-boson transverse momentum distribution*, Phys. Rev. D **87**, 014001 (2013) [arXiv:1201.5265].
- [38] N. Kidonakis, *Higher-order radiative corrections for  $b\bar{b} \rightarrow H^-W^+$* , Phys. Rev. D **97**, 034002 (2018) [arXiv:1704.08549].
- [39] N. Kidonakis and A. Toner,  *$N^3LO$  soft-gluon corrections in single-particle-inclusive kinematics and  $H^+H^-$  production*, JHEP **06**, 138 (2024) [arXiv:2404.00089].
- [40] S. Moch, J.A.M. Vermaseren, and A. Vogt, *The three-loop splitting functions in QCD: the non-singlet case*, Nucl. Phys. B **688**, 101 (2004) [arXiv:hep-ph/0403192].
- [41] H. Contopanagos, E. Laenen, and G. Sterman, *Sudakov factorization and resummation*, Nucl. Phys. B **484**, 303 (1997) [arXiv:hep-ph/9604313].
- [42] S. Moch and A. Vogt, *Higher-order soft corrections to lepton pair and Higgs boson production*, Phys. Lett. B **631**, 48 (2005) [arXiv:hep-ph/0508265].
- [43] E.G. Floratos, D.A. Ross, and C.T. Sachrajda, *Higher-order effects in asymptotically free gauge theories: The anomalous dimensions of Wilson operators*, Nucl. Phys. B **129**, 66 (1977) [(E) B **139**, 545 (1978)].
- [44] E.G. Floratos, D.A. Ross, and C.T. Sachrajda, *Higher-order effects in asymptotically free gauge theories: (II). Flavour singlet Wilson operators and coefficient functions*, Nucl. Phys. B **152**, 493 (1979).
- [45] A. Gonzalez-Arroyo, C. Lopez, and F.J. Yndurain, *Second-order contributions to the structure functions in deep inelastic scattering (I). Theoretical calculations*, Nucl. Phys. B **153**, 161 (1979).
- [46] G. Curci, W. Furmanski, and R. Petronzio, *Evolution of parton densities beyond leading order: The non-singlet case*, Nucl. Phys. B **175**, 27 (1980).
- [47] W. Furmanski and R. Petronzio, *Singlet parton densities beyond leading order*, Phys. Lett. B **97**, 437 (1980).
- [48] J. Kubar-Andre and F.E. Paige, *Gluon corrections to the Drell-Yan model*, Phys. Rev. D **19**, 221 (1979).

- [49] G. Altarelli, R.K. Ellis, and G. Martinelli, *Large perturbative corrections to the Drell-Yan process in QCD*, Nucl. Phys. B **157**, 461 (1979).
- [50] B. Humpert and W.L. van Neerven, *Infrared and mass regularization in AF field theories (II). QCD*, Nucl. Phys. B **184**, 225 (1981).
- [51] D.J. Gross and F. Wilczek, *Ultraviolet behavior of non-Abelian gauge theories*. Phys. Rev. Lett. **30**, 1343 (1973).
- [52] H.D. Politzer, *Reliable perturbative results for strong interactions?*, Phys. Rev. Lett. **30**, 1346 (1973).
- [53] G. 't Hooft, reported at the Marseille Conference, June 1972; see *When was asymptotic freedom discovered? or The rehabilitation of quantum field theory*, Nucl. Phys. B Proc. Suppl. **74**, 413 (1999) [arXiv:hep-ph/9808154].
- [54] T. Matsuura, S.C. van der Marck, and W.L. van Neerven, *The calculation of the second order soft and virtual contributions to the Drell-Yan cross section*, Nucl. Phys. B **319**, 570 (1989).
- [55] W.E. Caswell, *Asymptotic behavior of non-Abelian gauge theories to two-loop order*, Phys. Rev. Lett. **33**, 244 (1974).
- [56] D.R.T. Jones, *Two-loop diagrams in Yang-Mills theory*, Nucl. Phys. B **75**, 531 (1974).
- [57] E. Egorian and O.V. Tarasov, *Renormalization of Quantum Chromodynamics in the two-loop approximation in arbitrary gauge*, Teor. Mat. Fiz. **41**, 26 (1979), Theor. Math. Phys. **41**, 863 (1979).
- [58] J. Alwall *et al.*, *The automated computation of tree-level and next-to-leading order differential cross sections, and their matching to parton shower simulations*, JHEP **07**, 079 (2014) [arXiv:1405.0301].
- [59] R. Frederix, S. Frixione, V. Hirschi, D. Pagani, H.-S. Shao, and M. Zaro, *The automation of next-to-leading order electroweak calculations*, JHEP **07**, 185 (2018) [Erratum: JHEP **11**, 085 (2021)] [arXiv:1804.10017].
- [60] S. Bailey, T. Cridge, L.A. Harland-Lang, A.D. Martin, and R.S. Thorne, *Parton distributions from LHC, HERA, Tevatron and fixed target data: MSHT20 PDFs*, Eur. Phys. J. C **81**, 341 (2021) [arXiv:2012.04684].
- [61] J. McGowan, T. Cridge, L.A. Harland-Lang, and R.S. Thorne, *Approximate  $N^3$ LO parton distribution functions with theoretical uncertainties: MSHT20a $N^3$ LO PDFs*, Eur. Phys. J. C **83**, 185 (2023) [arXiv:2207.04739].
- [62] Particle Data Group, *Review of Particle Physics*, Phys. Rev. D **110**, 030001 (2024).
- [63] M. Grazzini, S. Kallweit, and M. Wiesemann, *Fully differential NNLO computations with MATRIX*, Eur. Phys. J. C **78**, 537 (2018) [arXiv:1711.06631].